In vitro membrane-inserted conformation of the cytochrome b_5 tail

Michael R. HANLON*, Rukhsana R. BEGUM†, Richard J. NEWBOLD†, David WHITFORD† and B. A. WALLACE*[1]

*Department of Crystallography, Birkbeck College, University of London, London WC1E 7HX, U.K., and †Laboratory of Structural Biochemistry, Molecular and Cellular Biology, Division of Biomedical Sciences, Queen Mary and Westfield College, University of London, London E1 4NS, U.K.

The cytochrome b_5 tail is a 43-residue membrane-embedded domain that is responsible for anchoring the catalytic domain of cytochrome b_5 to the endoplasmic reticulum membrane. Different models for the structure of the membrane domain of cytochrome b_5 have been proposed, including a helical hairpin and a single transmembrane helix. In the present study, CD spectroscopy was used to investigate the conformation of the tail in different environments, and as a function of temperature, with the goal of understanding the nature of the membrane-bound conformation. Whereas residue property profiling indicates that bending of a helix in the middle of the peptide might be possible, the experimental results in small unilamellar vesicles and lyso-phosphatidylcholine micelles are more consistent with a single transmembrane helix. Furthermore, although there is evidence for some refolding of the polypeptide with temperature, this is not consistent with a hairpin-to-transmembrane transition. Rather, it appears to represent an increase in helical content in fluid lipid environments, perhaps involving residues at the ends of the transmembrane segment.

Key words: circular dichroism spectroscopy, helix stability, integral membrane protein, phospholipid vesicles, secondary structure.

INTRODUCTION

Cytochrome b_5, a component of the microsomal membrane stearyl-CoA desaturase system, contains two distinct domains separated by a trypsin-sensitive region [1]. The larger, catalytic domain, of approx. 90 amino acid residues, transfers electrons to a variety of donors and acceptors within the endoplasmic reticulum (ER). The three-dimensional structure of this haem-binding domain has been characterized by crystallographic and NMR studies [2,3]. The other domain (the 'membrane-binding domain' or 'tail') of cytochrome b_5 is a much shorter (43 residues) hydrophobic fragment that anchors the globular domain to the ER membrane.

The sequences of cytochromes b_5 [4–13] from a number of mammalian sources have been determined, together with those of the yeast, chicken, tobacco and cauliflower proteins (Figure 1). Although the hydrophobic domain is less strongly conserved than the haem-binding domain, it is clear, especially for the mammalian proteins, that considerable identity also exists in the tail region. All of the tails exhibit a hydrophobic stretch of ~ 23 amino acids, of which the ten C-terminal residues are thought to be essential to the membrane-binding function [14].

Intact cytochrome b_5 requires detergent in order to remain in a monomeric state. In aqueous solutions, the hydrophobic domain promotes association into stable octameric complexes [15]. The potency of the tail in promoting association has been demonstrated by the observation that erythrocyte cytochrome b_5, with a haem-binding domain identical with that in the microsomal protein but lacking the hydrophobic domain, is a water-soluble protein that does not partition into membranes [16].

Studies of the interactions between cytochrome b_5 and artificial liposomes have shown that, *in vitro*, two different modes of binding can occur, depending upon the experimental conditions. A 'loose' form is obtained when cytochrome b_5 is mixed with preformed liposomes, and is characterized by the ability of the protein to exchange with added liposomes [17]. Alternatively, in the presence of detergent, a 'tight' form of binding is obtained, in which protein exchange is effectively prevented [18].

Two different conformations have been proposed for the membrane-binding domain: (1) a single membrane-spanning helix (Figure 2A), and (2) a hairpin-type structure [19], with two helical regions joined by a turn in the middle involving Pro-115; this structure is proposed to span only half of the bilayer thickness (Figure 2B). Digestion studies have indicated sensitivity of the last few residues to proteolysis, and, by implication, a single transmembrane helical topology in which the tail is accessible to the cytosol under tight binding conditions [20]. Cross-linking studies with photoactivatable cross-linkers have indicated that the hairpin conformation that spans only half the bilayer may be associated with the loose form, whereas the transmembrane arrangement is more consistent with the tight form [21]. Further support for the existence of two types of structure has come from fluorescence studies of the tail domain [22]: by measuring the changes in the quantum yield of Trp residues over the temperature range 10–70 °C, it was shown that the peptide could flip between two distinct conformations in palmitoyloleoylphosphatidylcholine vesicles. However, other cross-linking studies using a membrane-impermeant cross-linker have presented contradictory results to the above models, suggesting instead that the tight form is a hairpin conformation rather than a membrane-spanning conformation [18]. Furthermore, fluorescence quenching experiments [23] suggested that both the tight and loose forms are hairpin structures. Thus the structural identities of the two forms remain unclear.

CD spectroscopy and Fourier-transform IR spectroscopy have been used to probe the secondary structures of the membrane-binding domain [24–27] in various environments. These methods have produced a range of values, with β-sheet contents of up to 33 % and helical contents ranging from 43 to 61 %, depending on

Abbreviations used: DPPC, dipalmitoyl phosphatidylcholine, ER, endoplasmic reticulum; lysoPC, lysophosphatidylcholine (palmitoyl); NRMSD, normalized root-mean-square deviation; SUV, small unilamellar vesicle; TFE, 2,2,2-trifluoroethanol.

[1] To whom correspondence should be addressed (e-mail ubcg91c@ccs.bbk.ac.uk).

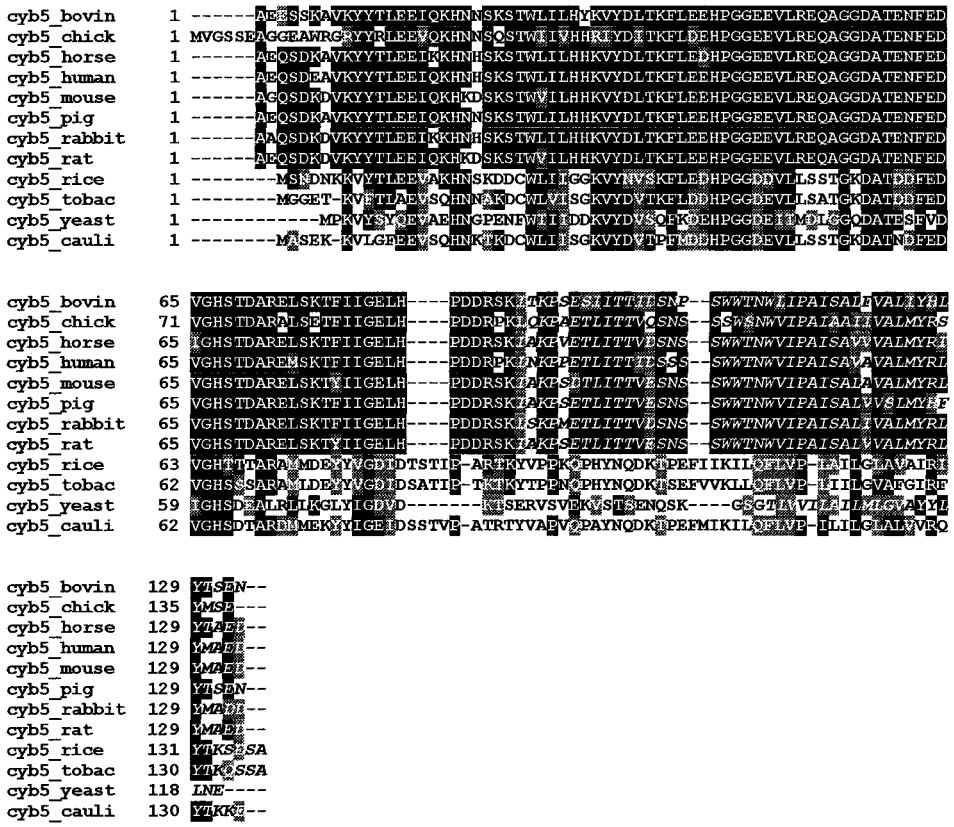

Figure 1 Multiple sequence alignment of cytochromes b_5 from a variety of sources

Conserved residues are shown in inverse (white lettering on a black background), and conservative substitutions are shaded. The extents of the tail domains are indicated by the italicized residues.

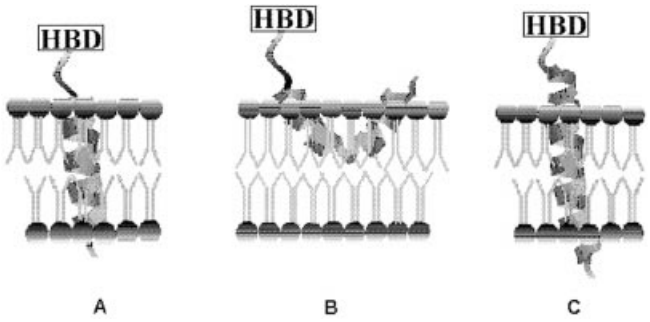

Figure 2 Proposed alternative topologies for the cytochrome b_5 tail

(**A**) Transmembrane model; (**B**) hairpin model; (**C**) transmembrane model at elevated temperatures, showing extension of the helical region. HBD, haem-binding domain.

the conditions and methods used. The helix contents obtained correspond to between 19 and 26 residues being in a helical conformation, which would be sufficient to span the membrane if they are in a single transmembrane helical segment. However, to date, the authors of the studies of secondary structure have tended to suggest that the results support a hairpin-type structure.

Studies of the hydrophobic domain using site-directed mutagenesis have provided additional information on the structure and topography of the membrane-binding fragment, although again all of these studies are not in complete agreement. Using a rabbit reticulocyte system, the translation of an mRNA encoding rat cytochrome b_5 in the presence of microsomes resulted in protein insertion into membranes [28]. The sensitivity of the protein to proteases was most compatible with a transmembrane conformation. Site-directed mutagenesis of Pro-115 to Ala did not alter the topology, although the affinity of peptide binding to membranes was diminished 2–3-fold. Mutagenesis of rat cytochrome b_5 showed that replacement of residues 104–125 with leucines yielded a protein that was capable of inserting into the ER membrane in a yeast expression system. However, this form of the protein showed impaired activity in reconstituted electron-transfer systems [29].

Further knowledge of the structure and folding of the membrane-binding domain of cytochrome b_5 will aid in our understanding of the role that the tail plays in targeting the protein to the correct membrane location and in governing its insertion into lipid bilayers. In the present study we have used CD spectroscopy to examine the conformation of the tail in different environments, as well as the effects of thermal changes on the conformation of the membrane-bound domain.

EXPERIMENTAL

Materials

The bovine cytochrome b_5 tail peptide (residues Ile-91 to Asn-133) was isolated by tryptic cleavage of a cloned full-length cytochrome b_5/thioredoxin fusion protein, as described previously [30]. On SDS/PAGE, the tail migrated as a single band

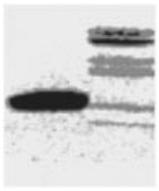

Figure 3 Polyacrylamide (25%)-gel electrophoresis of purified cytochrome b_5 tail stained with silver stain

Left lane, purified cytochrome b_5 tail; right lane, protein M_r standards (from top to bottom: 16900, 14400, 10700, 8100, 6200 and 2500).

with an apparent M_r of $\sim$ 5000 (Figure 3). MS produced a peak at 4964, consistent with the expected value for the peptide.

Sample preparation

The peptide solutions were prepared at concentrations of 0.66 mg/ml in the following solvents: methanol (spectrophotometric grade; Aldrich), 2,2,2-trifluoroethanol (TFE) (99+%; Aldrich), and n-propanol (AnalaR grade; Merck). Samples were vortexed briefly and then centrifuged at 12800 ***g*** for 5 min to remove any undissolved material.

For the palmitoyl lysophosphatidylcholine (lysoPC) samples, 2 mg of 1-palmitoyl-2-hydroxy-*sn*-glycero-2-phosphocholine (Avanti) was dissolved in 3 ml of distilled water. A 2.5 ml volume of this solution was added to 0.5 ml of the methanolic peptide solution prepared as described above. The mixture was sonicated for 2 min and then allowed to equilibrate at room temperature for 30 min prior to use.

The small unilamellar vesicle (SUV) samples were prepared as follows. The peptide was dissolved in methanol at a concentration of 0.66 mg/ml. Then 5 mg of dipalmitoyl phosphatidylcholine (DPPC) (Calbiochem) was dissolved in 1.0 ml of chloroform (spectrophotometric grade; Aldrich), to which was added 0.5 ml of the methanol solution of the peptide, providing a lipid/peptide molar ratio of 100:1. For baseline readings, the vesicles were prepared in the same manner but without peptide. The mixtures were vortexed briefly and dried under vacuum. Then 0.5 ml of deionized water was added and the jacketed sample was probe-sonicated at room temperature in 10 s bursts with an MSE Sonoprep 150 until the solution appeared opalescent, and then centrifuged at 12800 ***g***. The supernatant was retained for spectroscopic studies.

CD spectroscopy

Spectra were recorded using an Aviv 62ds spectropolarimeter with a detector acceptance angle of $\geqslant 90°$. The instrument had been calibrated previously for wavelength using benzene vapour, and for optical rotation using *d*-10-camphorsulphonic acid.

Spectra obtained in organic solvents and lysoPC were the result of averaging up to five scans for each preparation, collected at 10 °C. Dynode voltages for the first and last scans of a set were checked for consistency to ensure that no significant variation occurred during data collection. At least two independent preparations of each type of sample were examined.

Spectra obtained in vesicles were the result of averaging three scans taken at a given temperature. The temperature was varied between 10 °C and 60 °C in 10 °C steps, with 10 min equilibration periods between temperature changes for each set of spectra. The samples were cooled for 20 min after returning to 10 °C for the final set of scans.

Table 1 Secondary structural analyses of the cytochrome b_5 tail in alcohol solvents, lysoPC and DPPC

All values were obtained at 10 °C. NRMSD is a parameter indicating goodness-of-fit of the calculated structure to the experimental data.

	Secondary structure (%)				
Environment	Helix	Sheet	Turns	Other	NRMSD
Methanol	59	17	6	18	0.041
TFE	39	33	1	27	0.040
Propanol	60	0	18	22	0.036
LysoPC	68	0	10	22	0.034
DPPC	58	0	12	30	0.039

All spectra were collected over a wavelength range from 190 to 280 nm, using a step size of 0.2 nm in a 0.02 cm pathlength cell. Equivalent numbers of scans of the baseline samples (containing only solvent, lysoPC or vesicles) were obtained, averaged and subtracted from the averaged sample spectra. Spectra were then smoothed using a Savitsky–Golay filter [31]. Mean residue ellipticities were calculated using a mean residue weight of 116 for the polypeptide.

Analyses of secondary structure

All spectra were analysed using a least-squares curve-fitting procedure, with the fractions of secondary structure constrained to be non-negative and normalized to 100% [32]. The reference data set used was derived from 15 water-soluble proteins [33]. The helix length was varied in some of the calculations, but in general a helix length of 20 was used. Additionally, some spectra were analysed using an alternative reference data set [34] or an alternative calculation algorithm [35]. The qualities of the fits of the calculated secondary structures to the experimental data were determined using the normalized root-mean-square deviation (NRMSD) parameter [32]. NRMSD values of less than 0.1 usually mean that the calculated secondary structure corresponds well with the actual structure of the protein [34]. In the present study, all the NRMSD values were well below 0.1 (see Tables 1 and 2).

Although the NRMSD values for all samples were low, indicating a good correspondence between the calculated secondary structures and the actual structures, CD as a technique is most accurate in estimating helix content. As a result, most discussions of secondary structures in the present paper will concentrate on the helix content of the polypeptide. Although several different methods of analysis were used, only the results of one method [32] are reported in the Tables, as this method produced the lowest NRMSD values; all methods showed similar trends for the helical contents of the various samples.

Helix prediction and residue property profiling

A consensus prediction of the potential membrane helix-forming regions was obtained from the results of the following methods: TopPred2 [36], TMPred [37], TMHMM [38], SOSUI [39], HMMTOP [40] and PhdTM [41]. Residue property profiles were determined using scales of hydrophobicity [42], flexibility [43] and bulkiness [44]. Multiple sequence alignments were performed using ClustalW [45].

RESULTS

Secondary structure: environment-dependence

Cytochrome b_5 was expressed as a fusion product with thioredoxin and then purified after proteolytic cleavage to produce the isolated tail domain (Figure 3). The CD spectrum of the cytochrome b_5 tail in methanol (Figure 4A) exhibited a positive peak at 193 nm and negative peaks at 210 nm and 219 nm, with the lower-wavelength peak being the larger of the two negative peaks. In the TFE spectrum (Figure 4A), the peaks at 193 and 209 nm were both depressed in magnitude relative to the 220 nm peak (although the 220 nm peak was still larger than the 209 nm peak), and all were shifted slightly in position relative to the peaks in the methanol spectrum. In propanol (Figure 4A), the peaks were shifted towards higher wavelengths, and the two negative peaks were of approximately equal magnitude. Despite these minor differences, all three spectra are characteristic of a polypeptide with a significant amount of α-helical secondary structure.

Analyses of secondary structure (Table 1) indicated small but significant differences in the structures of the tail peptide in the three solvents, with that in propanol having the highest helix content ($\sim 60\,\%$). Surprisingly, the helix content in TFE, often considered a helix-inducing solvent, was the lowest ($\sim 40\,\%$). In propanol, there was no evidence for β-sheet structure, but there appeared to be a significant turn content (corresponding to up to eight residues, or one or two turns worth). In this case, the best fit to the data was obtained using a helix length of between 14 and 18 residues, suggesting (together with the turn content) that the structure in this solvent could be two short helices connected by a turn (as in the hairpin conformation). The other two solvents produced secondary structures with lower turn contents, but including some β-sheet, suggesting a somewhat different conformation.

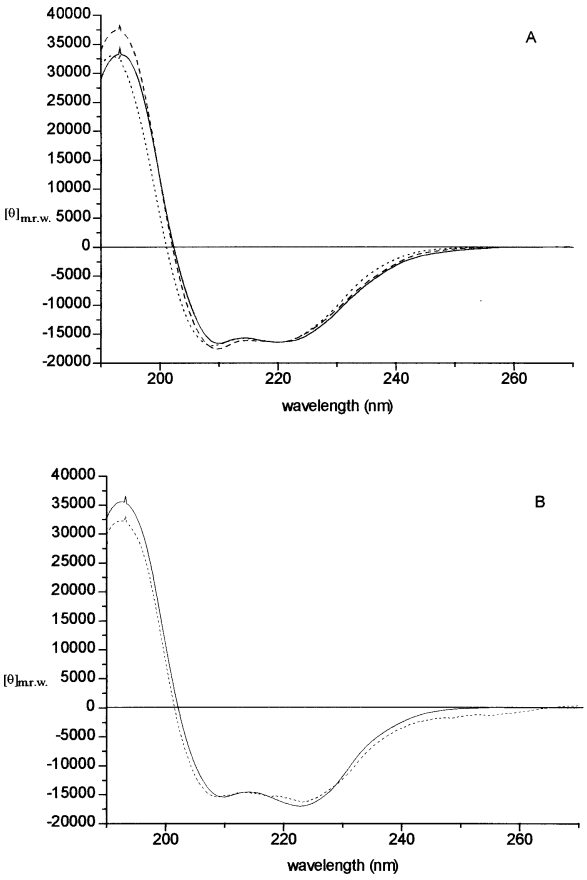

Figure 4 CD spectra of the cytochrome b_5 tail in (A) three different alcohols, and in (B) DPPC vesicles and lysoPC

(**A**) The alcohols were methanol (dashed line), TFE (dotted line) and propanol (solid line); spectra were obtained at at 10 °C. (**B**) Spectra were obtained for the cytochrome b_5 tail in DPPC vesicles at a lipid/protein ratio of 100:1 at 10 °C (dotted line), and in lysoPC at 10 °C (solid line).

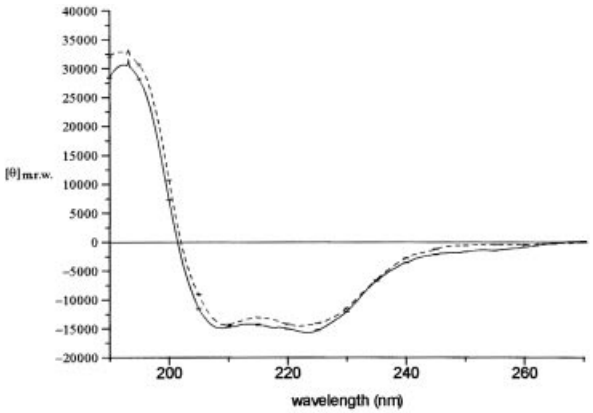

Figure 5 CD spectra of the cytochrome b_5 tail in DPPC vesicles as a function of temperature

Spectra were obtained at 10 °C (solid line) and at 60 °C (broken line). The error bars indicate the reproducibility of the data.

The CD spectrum of the tail peptide in lysoPC exhibited two negative peaks, at 209 and 223 nm, and a positive peak at 193 nm (Figure 4B). As we will see below, these positions corresponded closely to the positions found for the tail peptide in DPPC vesicles, but the highest-wavelength peak was shifted relative to any of the peaks in the alcohol solvents. The peak at 223 nm was slightly larger than that at 209 nm. The calculated secondary structure (Table 1) contained 68 % helix, somewhat higher than the helical values for any of the solvents.

Secondary structure in phospholipid vesicles

SUVs were used to obtain the spectra of the cytochrome b_5 tail as found in membranes, since it has been demonstrated that CD optical artifacts, such as absorption flattening and differential scattering, are minimal in these types of preparations [46,47]. The CD spectrum of the tail co-solubilized in DPPC vesicles at 10 °C displayed a positive peak at 193 nm and negative peaks at 209 nm and 223 nm (Figure 5). The magnitudes of the peaks at 209 and 223 nm were nearly equal (with the 223 nm peak being slightly larger than the 209 nm peak), as was the case for the peptide in propanol. The spectrum in DPPC at 60 °C (Figure 5) was most like that in lysoPC.

The spectrum of the cytochrome b_5 tail in DPPC is also characteristic of a polypeptide with a predominantly α-helical secondary structure. Analyses of secondary structure (Table 2) indicated a helix composition of $\sim 60\,\%$ in this environment, which would correspond to ~ 25 residues being in an α-helical type of conformation. Although there was not much variation with helix lengths greater than ten, the best fit to the data (lowest NRMSD) was obtained when an average helix length of $\geqslant 15$ was used in the calculations, suggesting that the helix may be

Table 2 Secondary structural analyses of the cytochrome b_5 tail in DPPC vesicles as a function of temperature

'→ 10' indicates the sample after cooling back to 10 °C.

	Secondary structure (%)				
Temperature (°C)	Helix	Sheet	Turns	Other	NRMSD
10	58	0	12	30	0.059
20	58	0	12	30	0.058
30	55	0	13	32	0.057
40	52	0	15	33	0.061
50	62	0	12	26	0.059
60	74	0	8	18	0.059
→ 10	56	1	10	33	0.050

Table 3 Predictions of transmembrane helix location

Method	Predicted segment (residue nos.)	Length (residues)
TopPred2	108–128	21
TMPred	109–126	18
TMHMM	108–130	23
SOSUI	108–129	22
HMMTOP	106–125	20
PHDTM	110–127	18

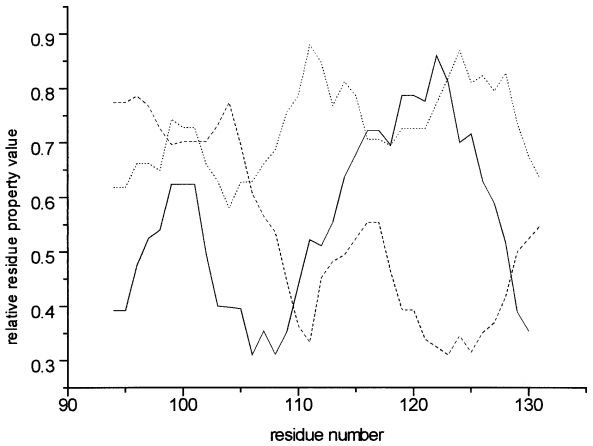

Figure 6 Comparison of predicted residue properties as a function of sequence

The properties shown are hydrophobicity (solid line), flexibility (dashed line) and bulkiness (dotted line).

present as a single element rather than as two shorter helices. A single helix of 25 residues would be of a comparable length to transmembrane helices found in other membrane proteins and sufficient to span the bilayer. Hence we propose, based on our CD data, that the cytochrome b_5 tail adopts a single transmembrane helical structure, although we cannot completely exclude other topologies.

The CD results in DPPC in the present study do not support the assignment of any β-sheet structure to the peptide in membranes, in contrast with the suggested value of 25 % based on previous CD studies [24]. However, those earlier CD studies were carried out under conditions where considerable differential scattering, and perhaps absorption flattening, was present but not corrected for, distortions which tend to depress the lower-wavelength peaks and artificially increase the calculated sheet content. In the present studies, the detector geometry used minimizes scattering effects [48], and the protein/lipid ratios and vesicle sizes minimize the absorption flattening effects [46]. The results show clearly that the preponderance of secondary structure is helical.

Predictions of the secondary structure of the potential membrane-spanning helices in the sequence (Table 3) suggest the presence of a single helix of $\sim$ 20 residues in length, centred at around residues 116–117, a result consistent with the hydrophobicity plot (Figure 6). Previous attempts at secondary structure prediction [24] had suggested that only $\sim$ 11 amino acids, i.e. the residues between positions 115 and 125, would form a helical structure, with most of the rest of the polypeptide being either turn or sheet. Those calculations were probably not very reliable, because the Chou and Fasman [49] method used employed parameters that were developed for soluble proteins and have been shown to be poorly suited for the prediction of membrane proteins [50]. However, the methods adopted here employed algorithms specifically intended for the prediction of membrane-spanning segments, and suggest that the potential membrane helix may be located between residues 108 and 128, a result in close agreement with the hydrophilicity analysis by Pedrazzini et al. [51] of the sequence of the rabbit cytochrome b_5 tail. These calculations of helix length are consistent with the helical content determined from the CD data in vesicles in the present study, and again indicate that the most probable conformation is a single transmembrane helix.

Thermal-induced conformational changes in vesicles

The conformation of the tail in DPPC vesicles was investigated as a function of temperature. Reversible changes were observed in all three peaks (Figure 5). These corresponded to a reversible increase (by about 15 %) in the helix content with temperature (Table 2). Athough not strictly related to the phase-state transition temperature of the lipids, these observations could suggest that, as the lipids become more fluid, the protein experiences a flexible environment in which it can undergo a conformational change.

Could these temperature-dependence data shed any light on the two alternative topology models that have been proposed for this peptide (Figure 2)? In the transmembrane model (Figure 2A), there is a single helix that spans the bilayer. In the hairpin model (Figure 2B), the polypeptide contains a sharp bend around Pro-115, effectively resulting in two short helices. A kink of 26° at Pro-115 has been proposed for the latter model, due to the tendency of this type of residue to induce bends in helices [52]. However, observations of the proline residues in the transmembrane regions of other membrane proteins (e.g. bacteriorhodopsin [53]) have demonstrated that such a large kink is not obligatory around prolines. Site-directed mutagenesis of this proline in the cytochrome b_5 tail to an alanine appears to have little effect on the integrity of the peptide in membranes [28]. However, property profiling of the tail sequence (Figure 6) shows deviations in both the bulkiness and flexibility near the Pro-115 residue, which could be consistent with a bend. A possible reconciliation of the alternative topologies is a two-state model of membrane binding [28]. Initial spontaneous insertion of the hairpin configuration would be followed by translocation of the membrane-spanning segment in conjunction with a *cis* → *trans* isomerization of the Ile-114–Pro-115 peptide bond to

form a single transmembrane helix. Thus the 'loose' binding mode would permit exchange of the peptide tail between vesicles [17], while interconversion produces the more energetically favourable and stable 'tight' configuration.

Although, superficially, the temperature-dependent CD change observed might seem to be due to a hairpin-to-transmembrane transition, such an explanation is unlikely for several reasons. (1) The data, even at low temperatures, are more consistent with a transmembrane conformation than a hairpin. (2) The changes involve an increase in helix and a concomitant decrease in disordered structure. For the hairpin-to-transmembrane change, only a very small change ($< 7\%$) in helix content would be expected (it just involves two short helices becoming one long one, with at most three residues changing conformation). (3) The hairpin-to-transmembrane conformational change is unlikely to be reversible under these conditions. Re-orientation to a hairpin following a decrease in temperature from the transmembrane state, where the polypeptide interacts with the bilayer interface on both ends, would probably be energetically unfavourable. A more likely explanation for the increase in helix content seen is that it is due to the ends of the transmembrane helix near the membrane interface becoming more ordered as the lipid fluidity becomes less restrictive (Figure 2C), similar to what has been suggested for bacteriorhodopsin on refolding [54].

The secondary structure in DPPC vesicles at high temperatures was very similar to that in lysoPC micelles (Table 1). This suggests that the environment in the detergent may be comparable with that in a fluid lipid membrane, due to a similar lack of constraining factors. Furthermore, it appears that, in this detergent, the structure is also in the tight conformation.

DISCUSSION

The spectra of the cytochrome b_5 tail obtained in the three alcohol solvents exhibited significant differences. Solvent-induced changes in the CD spectra of peptides in non-aqueous environments may be divided into primary and secondary effects [55]. The former appear as alterations in the waveforms (relative peak magnitudes) and subsequently lead to significant differences in the secondary structure analyses, whereas the latter result in shifts in the positions of the peaks, without significant changes in the waveforms, but can often also be detected as deteriorations in the NRMSD fits. Examination of the spectra in Figure 4 suggests that primary effects predominate in these cases, as the changes are not only in the positions of peak maxima, but also in the relative peak intensities, and in the calculated secondary structures.

Alcohols tend to have two major types of effects on the conformations of peptides and proteins: (1) the stabilization/induction of local secondary structure (particularly α-helix), and (2) the disruption of tertiary structure. Decreasing the polarity of the solvent tends to weaken the hydrophobic interactions that help to maintain tertiary structure, while strengthening the intramolecular hydrogen bonds involved in secondary structural elements. The relative dielectric constants of the three alcohols [56] would suggest an effectiveness in inducing structural transitions that should be (in descending order): methanol > TFE > propanol. If we take the CD spectrum in DPPC (Figure 4B) to be the 'native' structure, then we might order the apparent disruption of tertiary structure, as displayed by changes in the α-helical content of the peptide from the CD data, as propanol > methanol > TFE. This bears no correlation with the order of effectiveness cited above. However, there is probably more involved here than just relative polarities in inducing these primary effects. The group-additive contribution of a wide range of alcohols has been investigated in this context [57], the results of which suggest a revised, and, in this case, slightly more correlated, order of effectiveness, i.e. methanol > propanol > TFE. It has been suggested that the ability of TFE to provide hydrophobic surfaces may result in an environment reminiscent of the hydrophobic cores of membranes [58], but this does not seem to be the case for the cytochrome b_5 tail. Interestingly, propanol has the largest accessible surface area of the three alcohols studied here, and is also the most hydrophobic. This might offer some explanation for the apparent better maintenance of structure in this solvent. If so, this finding addresses an important additional objective of the present study, which was to identify a possible membrane-mimetic solvent environment for one form of the cytochrome b_5 tail in which other conformational studies, such as NMR spectroscopy or crystallization, could be performed.

The authors of earlier CD studies [25] have stated that results similar to those in liposomes were obtained in 0.4% sodium deoxycholate, 25–75% propanol and 50% TFE for the cytochrome b_5 tail, but, upon inspection of the spectra in that study, it is clear that the structures are quite different in these different environments. The authors estimated that the vesicle spectrum was representative of a protein with 45% helix and 25% sheet content. However, as noted above, the spectra were uncorrected for scattering effects, which tend to decrease the apparent helix content and enhance the apparent sheet content. In contrast, Fourier-transform IR studies [27] suggested a helix content of 52–61% for the tail in different types of vesicles, very similar to the results reported here. In the present study, the co-solubilization procedure used for incorporation into vesicles would appear to be producing the 'tight' form of the structure with a high helix content, as is the case in the lysoPC detergent.

The results of the present study are more compatible with the tight binding configuration being a single transmembrane-spanning helix. This is consistent with earlier neutron diffraction studies [59], which indicated that the tail penetrates deep into the lipid bilayer, but is at odds with low-angle X-ray scattering studies [60], which suggested that the tail only spans one-half of the bilayer (as it would in a hairpin). Fluorescence energy transfer measurements using modified lipids containing 9-anthroyloxy fatty acid probes showed that most of the fluorescence was associated with one of the three conserved Trp residues and that this residue was buried approximately 20 Å from the membrane surface in dimyristoyl phosphatidylcholine vesicles [61], a result that would be compatible with either a transmembrane structure or a hairpin. A later fluorescence energy transfer study [62] using a mutant version of the cytochrome b_5 tail with a single Trp suggested that it did not adopt a hairpin conformation. In addition, different proteolysis studies [63,17] have produced contradictory results, each being consistent with one of the different models.

If we look carefully, however, at the experimental procedures used in the various studies, it would appear that most of the discrepancies in results obtained using different techniques *in vitro* are due to the use of different methods for incorporation or binding of the cytochrome b_5 tail to membranes. When the protein is co-solubilized or sonicated with the lipid, or incorporated by a method such as detergent dialysis, it appears to result in the transmembrane configuration. However, in general, if the protein has been bound to the surface of the membrane initially, even after heat treatment, it only seems to span half the membrane (perhaps as a hairpin). The present study does not provide any evidence in support of a hairpin-to-transmembrane transition, but rather suggests that a more fluid membrane environment does permit some refolding of the protein. It also

demonstrates that the tight form of the tail has a more helical overall structure than seen previously for the loose form of the molecule.

The question still remains: how do these results relate to the form that is found *in vivo*? Insertion of cytochrome b_5 into the ER membrane occurs without the involvement of the signal recognition particle complex [64] and in the absence of a cleaved N-terminal signal sequence [65]. It is clear that the tail contains membrane-targeting information from the demonstration that, in chimaeric constructs, this sequence is able to direct 'foreign' proteins specifically to the ER membrane [14]. Various results from membrane-targeting studies suggest that its membrane localization is not merely due to a non-specific hydrophobic interaction, but may involve a receptor-mediated insertion pathway in the ER [14]. Mutagenesis studies have specifically implicated the final ten residues of the hydrophobic domain as being the targeting sequence. Furthermore, in a rabbit reticulocyte system, translation in the presence of microsomes resulted in protein insertion into membranes in a conformation that was sensitive to proteases, in a manner that suggested a transmembrane conformation. These studies tend to support the conclusion that the tight conformation is the form that is found in biological membranes.

No examples of stable integral membrane protein structures that span only one-half of the bilayer in a hairpin conformation have been identified in the high-resolution X-ray structures of membrane proteins determined to date. This may be because the presence of a turn in the middle of a structure would result in a lower number of polypeptide backbone hydrogen bonds in the transmembrane region, a situation which would be energetically less favourable than if all the residues were in a helical conformation. It appears that the cytochrome b_5 tail does not represent a counter-example to this pattern.

In conclusion, the present CD study of the membrane-inserted form of the cytochrome b_5 tail favours the conclusion that the tight form of the protein is a transmembrane helical structure. Temperature-dependence studies suggest that a conformational change occurs associated with the tail being in a fluid environment that allows maximization of the helical nature of the polypeptide in membranes.

M.R.H. and R.R.B. were supported by BBSRC studentships, and R. J. N. was supported by a project grant from the BBSRC.

REFERENCES

1 Spatz, L. and Strittmatter, P. (1971) Form of cytochrome b_5 that contains an additional hydrophobic sequence of forty amino acid residues. Proc. Natl. Acad. Sci. U.S.A. **68**, 1042–1046

2 Durley, R. and Mathews, F. S. (1996) Refinement and structural analysis of bovine cytochrome b_5 at 1.5 Å resolution. Acta. Crystallogr. **D52**, 65–76

3 Muskett, F. W., Kelly, G. P. and Whitford, D. (1996) The solution structure of bovine ferricytochrome b_5 determined using heteronuclear NMR methods. J. Mol. Biol. **258**, 172–189

4 Cristiano, R. J. and Steggles, A. W. (1989) The complete nucleotide sequence of bovine liver cytochrome b_5 mRNA. Nucleic Acids Res. **17**, 799

5 Zhang, H. and Somerville, C. (1988) The primary structure of chicken liver cytochrome b_5 deduced from the DNA sequence of a cDNA clone. Arch. Biochem. Biophys. **264**, 343–347

6 Ozols, J., Gerard, C. and Nobrega, F. G. (1976) Proteolytic cleavage of horse liver cytochrome b_5. Primary structure of the heme-containing moiety. J. Biol. Chem. **251**, 6767–6774

7 Yoo, M. and Steggles, A. W. (1988) The complete nucleotide sequence of human liver cytochrome b_5 mRNA. Biochem. Biophys. Res. Commun. **156**, 576–580

8 Vandermark, P. K. and Steggles, A. W. (1997) The isolation and characterization of the soluble and membrane-bound porcine cytochrome b5 cDNAs. Biochim. Biophys. Acta. **240**, 80–83

9 Ozols, J. (1970) Amino acid sequence of rabbit liver microsomal cytochrome b_5. J. Biol. Chem. **245**, 4863–4874

10 Ozols, J. and Heinemann, F. S. (1982) Chemical structure of rat liver cytochrome b_5. Isolation of peptides by high pressure liquid chromatography. Biochim. Biophys. Acta. **704**, 163–173

11 Smith, M. A., Stobart, A. K., Shewry, P. R. and Napier, J. A. (1994) Tobacco cytochrome b_5: cDNA isolation, expression analysis and in vitro protein targeting. Plant Mol. Biol. **25**, 527–537

12 Truan, G., Epinat, J.-C., Rougeulle, C., Cullin, C. and Pompon, D. (1994) Cloning and characterization of a yeast cytochrome b_5-encoding gene which suppresses ketoconazole hypersensitivity in a NADPH-P-450 reductase-deficient strain. Gene **142**, 123–127

13 Kearns, E. V., Keck, P. and Somerville, C. R. (1992) Nucleotide sequence of cDNA for cytochrome b_5 from cauliflower (Brassica oleracea L.). Plant Physiol. **99**, 1254–1257

14 Mitoma, J. and Ito, A. (1992) The carboxy-terminal 10 amino acid residues of cytochrome b_5 are necessary for its targeting to the endoplasmic reticulum. EMBO J. **11**, 4197–4203

15 Ito, A. and Sato, R. (1968) Purification by means of detergents and properties of cytochrome b_5 from liver microsomes. J. Biol. Chem. **243**, 4922–4925

16 Hultquist, D. E. and Passon, P. G. (1971) Catalysis of methaemoglobin reduction by erythrocyte cytochrome b_5 and cytochrome b_5 reductase. Nature (London) **229**, 252–254

17 Enoch, H., Fleming, P. J. and Strittmatter, P. (1979) The binding of cytochrome b_5 to phospholipid vesicles and biological membranes. J. Biol. Chem. **254**, 6483–6488

18 Arinc, E., Rzepecki, L. M. and Strittmatter, P. (1987) Topography of the C-terminus of cytochrome-b_5 tightly bound to dimyristoylphosphatidylcholine vesicles. J. Biol. Chem. **262**, 15563–15567

19 Visser, L., Robinson, N. C. and Tanford, C. (1975) The two domain structure of cytochrome b_5 in deoxycholate solution. Biochemistry **14**, 1194–1199

20 Kuroda, K., Kinoshita, J.-Y., Honsho, M., Mitoma, J.-Y. and Ito, A (1996) *In situ* topology of cytochrome b_5 in the endoplasmic reticulum. J. Biochem. (Tokyo). **120**, 828–833

21 Takagaki, Y., Radhakrishnan, R., Wirtz, K. W. A. and Khorana, H. G. (1983) The membrane-embedded segment of cytochrome-b_5 as studied by cross-linking with photoactivatable phospholipids. 2. The nontransferable form. J. Biol. Chem. **258**, 9136–9142

22 Ladokhin, A. S., Wang, L., Steggles, A. W., Malak, H. and Holloway, P. W. (1993) Fluorescence study of a temperature-induced conversion from the loose to the tight binding form of membrane-bound cytochrome b_5. Biochemistry **32**, 6951–6956

23 Tennyson, J. and Holloway, P. W. (1986) Fluorescence studies of cytochrome b_5 topography – incorporation of cytochrome b_5 into brominated phosphatidylcholine vesicles by deoxycholate. J. Biol. Chem. **261**, 14196–14200

24 Fleming, P. J., Dailey, H. A., Corcoran, D. and Strittmatter, P. (1978) The primary structure of the non polar segment of bovine cytochrome b_5. J. Biol. Chem. **253**, 5369–5372

25 Dailey, H. A. and Strittmatter, P. (1978) Structural and functional properties of the membrane binding segment of cytochrome b_5. J. Biol. Chem. **253**, 8203–8209

26 Holloway, P. W. and Mantsch, H. H. (1989) Structure of cytochrome b_5 in solution by fourier-transform infrared-spectroscopy. Biochemistry **28**, 931–935

27 Holloway, P. W. and Buchheit, C. (1990) Topography of the membrane-binding domain of cytochrome b_5 in lipids by fourier-transform infrared-spectroscopy. Biochemistry **29**, 9631–9637

28 Vergeres, G., Ramsden, J. and Waskell, L. (1995) The carboxyl-terminus of the membrane-binding domain of cytochrome b_5 spans the bilayer of the endoplasmic reticulum. J. Biol. Chem. **270**, 3414–3422

29 Wu, F. F., Vergeres, G. and Waskell, L. (1994) Kinetics of the reduction of cytochrome b_5 with mutations in its membrane-binding domain. Arch. Biochem. Biophys. **308**, 380–386

30 Begum, R. R., Newbold, R. J. and Whitford, D. (2000) Purification of the membrane binding domain of cytochrome b_5 by immobilized nickel chelate chromatography. J. Chromatogr. **737**, 119–130

31 Savitsky, A. and Golay, M. J. E. (1964) Smoothing and differentiation of data by simplified least squares procedures. Anal. Chem. **36**, 1627–1639

32 Mao, D., Wachter, E. and Wallace, B. A. (1982) Folding of the mitochondrial proton adenosine-triphosphatase proteolipid channel in phospholipid vesicles. Biochemistry **21**, 4960–4968

33 Chang, C. T., Wu, C. C. and Yang, J. T. (1978) Circular dichroic analysis of protein conformation : inclusion of the β-turns. Anal. Biochem. **91**, 13–31

34 Brahms, S. and Brahms, J. (1980) Determination of protein secondary structure in solution by vacuum ultraviolet circular dichroism. J. Mol. Biol. **138**, 149–178

35 Hennessey, Jr, J. P. and Johnson, Jr, W. C. (1982) Experimental errors and their effect on analyzing circular-dichroism spectra of proteins. Anal. Biochem. **125**, 177–188

36 von Heijne, G. (1992) Membrane protein structure prediction, hydrophobicity analysis and the positive-inside rule. J. Mol. Biol. **225**, 487–494

37 Hofmann, K. and Stoffel, W. (1992) Profilegraph – An interactive graphical tool for protein sequence analysis. Comput. Appl. Biosci. **8**, 331–337
38 Sonnhammer, E. L. L., von Heijne, G. and Knogh, A. (1998) A Hidden Markov Model for predicting transmembrane helices in protein sequences. In Proceedings of the Sixth International Conference on Intelligent Systems for Molecular Biology, pp. 175–182, AAAI Press, Menlo Park, CA
39 Hirokawa, T., BoonChieng, S. and Mitaku, S. (1998) SOSUI: classification and secondary structure prediction system for membrane proteins. Bioinformatics **14**, 378–379
40 Tusnady, G. E. and Simon, I. (1998) Principles governing amino acid composition of integral membrane proteins: Application to topology prediction. J. Mol. Biol. **283**, 489–506
41 Rost, B., Casadio, R., Fariselli, P. and Sander, C. (1995) Transmembrane helices predicted at 95 percent accuracy. Protein Sci. **4**, 521–533
42 Kyte, J. and Doolittle, R. F. (1982) A simple method for displaying the hydropathic character of a protein. J. Mol. Biol. **157**, 105–132
43 Bhaskaran, R. and Ponnuswamy, P. K. (1988) Positional flexibilities of amino acid residues in globular proteins. Int. J. Peptide Protein Res. **32**, 241–255
44 Zimmerman, J. M., Eliezer, N. and Simha, R. (1968) The characterization of amino acid sequences in proteins by statistical methods. J. Theor. Biol. **21**, 170–201
45 Thompson, J. D., Higgins, D. G. and Gibson, T. J. (1994) ClustalW: improving the sensitivity of progressive multiple sequence alignments through sequence weighting, position specific gap penalties and weight matrix choice. Nucleic Acids Res. **22**, 4673–4680
46 Mao, D. and Wallace, B. A. (1984) Differential light scattering and absorption flattening optical effects are minimal in the circular dichroism spectra of small unilamellar vesicles. Biochemistry **23**, 2667–2673
47 Wallace, B. A. and Teeters, C. L. (1987) Differential absorption flattening optical effects are significant in the circular-dichroism spectra of large membrane fragments. Biochemistry **26**, 65–70
48 Schneider, A. S. and Harmatz, D. (1976) An experimental method correcting for absorption flattening and scattering on suspensions of absorbing particles: circular dichroism and absorption spectra of hemoglobin in situ in red blood cells. Biochemistry **15**, 4158–4162
49 Chou, P. Y. and Fasman, G. D. (1974) Prediction of protein conformation. Biochemistry **13**, 222–245
50 Wallace, B. A., Cascio, M. and Mielke, D. L. (1986) Membrane protein secondary structure prediction – an evaluation of empirical methods. Proc. Natl. Acad. Sci. U.S.A. **83**, 9423–9427
51 Pedrazzini, E., Villa, A. and Borgese, N. (1996) A mutant cytochrome b_5 with a lengthened membrane anchor escapes from the endoplasmic reticulum and reaches the plasma membrane. Proc. Natl. Acad. Sci. U.S.A. **93**, 4207–4212
52 Vergeres, G. and Waskell, L. (1995) Cytochrome b_5, its functions, structure and membrane topology. Biochimie **77**, 604–620
53 Luecke, H., Richter, H. T. and Lanyi, J. K. (1998) Proton transfer pathways in bacteriorhodopsin at 2.3 Å resolution. Science **280**, 1934–1937
54 Riley, M. L., Wallace, B. A., Flitsch, S. L. and Booth, P. J. (1997) Slow α-helix formation during folding of a membrane protein. Biochemistry **36**, 192–196
55 Chen, Y. and Wallace, B. A. (1997) Secondary solvent effects on the circular dichroism spectra of polypeptides in non-aqueous environments: influence of polarization effects on the far ultraviolet spectra of alamethicin. Biophys. Chem. **65**, 65–74
56 Lide, D. R. (ed.) (1995) CRC Handbook of Chemistry and Physics 76th edn. pp. 6-159–6-192, CRC Press, Boca Raton
57 Hirota, N., Mizuno, K. and Goto, Y. (1998) Group additive contributions to the alcohol-induced α-helix formation of melittin: Implication for the mechanism of the alcohol effects on proteins. J. Mol. Biol. **275**, 365–378
58 Gast, K., Zirwer, D., Muller-Frohne, M. and Damaschun, G. (1998) Compactness of the kinetic molten globule of bovine alpha-lactalbumin: A dynamic light scattering study. Protein Sci. **8**, 625–634
59 Gogol, E. P. and Engelman, D. M. (1984) Neutron scattering shows that cytochrome b_5 penetrates deeply into the lipid bilayer. Biophys. J. **46**, 491–495
60 Chester, D. W., Skita, V., Young, H. S., Mavromoustakos, T. and Strittmatter, P. (1992) Bilayer structure and physical dynamics of the cytochrome b_5 dimyristoylphosphatidylcholine interaction. Biophys. J. **61**, 1224–1243
61 Kleinfeld, A. M. and Lukacovic, M. F. (1985) Energy transfer study of cytochrome b_5 using the anthroyloxy fatty acid membrane probes. Biochemistry **24**, 1883–1890
62 Ladokhin, A. S., Wang, L., Steggles, A. W. and Holloway, P. W. (1991) Fluorescence study of a mutant cytochrome b_5 with a single tryptophan in the membrane-binding domain. Biochemistry **30**, 10200–10206
63 Ozols, J. (1989) Structure of cytochrome b_5 and its topology in the microsomal membrane. Biochim. Biophys. Acta **997**, 121–130
64 Okada, Y., Frey, A. B., Guenthner, T. M., Oesch, F., Sabatini, D. D. and Kreibich, G. (1982) Studies on the biosynthesis of microsomal membrane proteins – site of synthesis and mode of insertion of cytochrome b_5, cytochrome b_5 reductase, cytochrome p450 and epoxide hydrolase. Eur. J. Biochem. **122**, 393–402
65 Anderson, D. J., Mostov, K. E. and Blobel, G. (1983) Mechanisms of integration of de novo synthesized polypeptides into membranes – signal recogntiion particle is required for integration into microsomal membranes of calcium ATPase and of lensMP26 but not of cytochrome b_5. Proc. Natl. Acad. Sci. U.S.A. **80**, 7249–7253

Received 30 May 2000/8 August 2000; accepted 1 September 2000